Green Ultrasound Assisted Synthesis of N^2,N^4,N^6-tris ((Pyridin-2-ylamino) methyl)-1, 3,5-triazine-2,4,6-Triamine as Effective Corrosion Inhibitor for Mild Steel in 1 M Hydrochloric Acid Medium

Chandrabhan Verma[1], M.A. Quraishi[*], E.E. Ebenso[2]

[1]Department of Applied Chemistry, Indian Institute of Technology, Banaras Hindu University, Varanasi-221005, India
[2] Material Science Innovation & Modelling (MaSIM) Research Focus Area, Faculty of Agriculture, Science and Technology, North-West University (Mafikeng Campus), Private Bag X2046, Mmabatho 2735, South Africa
[*]E-mail: maquraishi.apc@itbhu.ac.in

An new corrosion inhibitor namely N^2,N^4,N^6-tris ((Pyridin-2-ylamino) methyl)-1, 3,5-triazine-2,4,6-triamine (INH) was synthesized using green ultrasound technique and its inhibition property on corrosion of mild steel has been studied using gravimetric measurement, Potentiodynamic polarization , electrochemical impedance spectroscopy (EIS) and linear polarization (LR) resistance . Potentiodynamic polarization measurements reveal that this compound effectively suppressed corrosion of mild steel in acid solution and acts as mixed-type inhibitor. EIS plots indicates that the addition of inhibitor increases the charge-transfer resistance (R_{ct}) and decreases the double-layer capacitance (C_{dl}) of the corrosion process this reveals that investigated inhibitor inhibits mild steel corrosion by adsorption on its surface. The adsorption of inhibitor on the mild steel surface obeys Langmuir adsorption isotherm.

1. INTRODUCTION

The Mild steel is a reactive material and prone to corrosion in acid media [1].The process of corrosive degradation of materials is not only of great complexity but also of enormous economic importance. During past few years, a variety of N-heterocyclic compounds have been reported as effective corrosion inhibitors for mild steel in acid solutions [2-14]. The choice of these compounds as

corrosion inhibitors is based on the consideration that these compounds contain conjugated π-electrons and heteroatoms which provide them a better coordination and adsorption property. The adsorption of these compounds is influenced by the electronic structure of inhibiting molecules, steric factor, aromatic and electron density at donor site, presence of functional group such as –CHO, –N=N, R–OH etc. molecular area and molecular weight of the inhibitor molecule [15-18].

In our present work, we have synthesized a N-heterocyclic compound, namely N^2,N^4,N^6-tris ((Pyridin-2-ylamino) methyl)-1, 3,5-triazine-2,4,6-triamine and investigated its corrosion inhibition properties using weight-loss, Potentiodynamic polarization, linear polarization resistance (*LPR*) and electrochemical impedance spectroscopy (*EIS*) methods . Several isotherms were also tested for their relevance to describe the adsorption behavior of investigated inhibitor.

2. EXPERIMENTAL

2.1 Inhibitor:

The inhibitor N^2,N^4,N^6-tris((Pyridin-2-ylamino)methyl)-1,3,5-triazine-2,4,6-triamine inhibitor was synthesized by modified method using ultrasonication technique. Melamine, Formaldehyde and 2-aminopyridine in a molar ratio of 1:3:3 were taken in ethanol and sonicated for 30-35 minutes (84% yield). The synthesis was also achieved by refluxing this reaction mixture for 5-6 hours in ethanol (69% yield). The solid product obtained by cooling the reaction medium was recrystallized in ethanol to obtained pure product. The purity of the product was confirmed by thin-layer chromatography in ethyl acetate/n-hexane (4:6) as developing solvent using the Silica Plate (TLC Plates−Aluminum (Al) Silica) and it was characterized by proton nuclear magnetic resonance (^{1}HNMR) and infra-ied (FT-IR) spectroscopy..The solid product decomposed above 300^0C , IR-(KBr, cm^{-1}): v 3384, 2957, 1599, 1557, 1488, 1440,1308,1194,1094, 884,871,814,773,738,619, ^{1}H NMR-(CDCl$_3$, 300 MHz): δ 4.81(s, 2H), δ 6.56(m, 1H), δ7.37 (d,1H), δ 7.57(d, 1H), 7.59(m, 1H), δ 8.10(d,1H). The synthetic route is given scheme in 1.
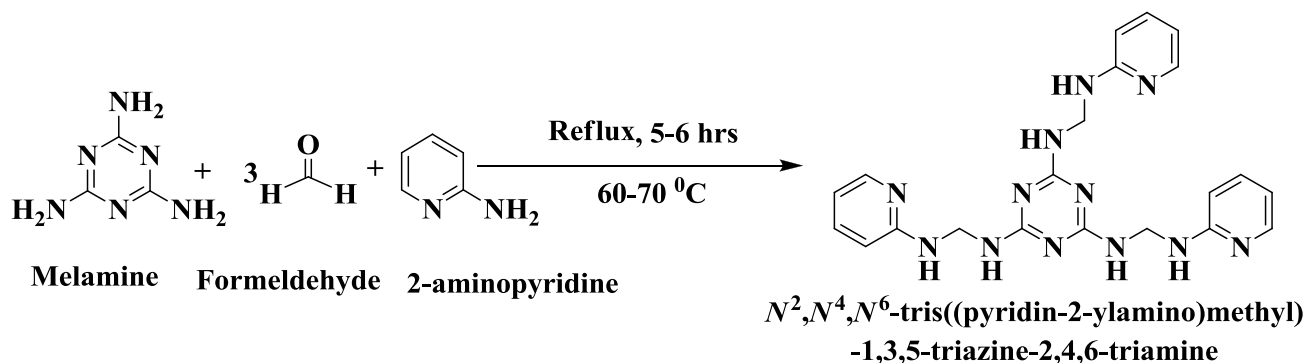
Scheme1. *Synthetic route of* N^2,N^4,N^6-tris((Pyridin-2-ylamino)methyl)-1,3,5-triazine-2,4,6-triamine

2.2 Corrosion measurements

The mild steel specimens, having composition (wt %) Fe 99.30%, C 0.076%, Si 0.026%, Mn 0.192%, P 0.012%, Cr 0.050%, Ni 0.050%, Al 0.023%, and Cu 0.135%, were abraded successively with emery papers from 600 to 1200 mesh/in grade. The mild steel specimen washed with double distilled water, degreased with acetone and finally dried in hot air blower. The working electrode (WE) was a 7.0 cm long stem (isolated with epoxy resin) to provide an exposed surface area of 1.0 cm^2 for electrochemical measurements and   dimension 2.5 × 2.0 × 0.025 cm^3 were used in weight loss experiments. The test solution 1 M HCl prepared from analytical reagent grade reagent (37 % HCl) and double distilled water.

2.3. Weight loss method

The weight loss measurements were carried out by standard method as described earlier [19].The inhibition efficiency (η%) and surface coverage (θ) were calculated by using the following equations:

$$\eta\% = \frac{C_R - C_{R(i)}}{C_R} \times 100$$

(1)

$$\theta = \frac{C_R - C_{R(i)}}{C_R}$$

(2)

where C_R and $C_{R(i)}$ are the corrosion rate values in absence and presence of inhibitor respectively. The corrosion rate (C_R) of mild steel in acidic medium was calculated by using following equation:

$$C_R = \frac{W}{At}$$

(3)

where, *W* is weight loss of mild steel specimens (mg)*, A* is the area of the specimen (cm^2) and *t* is the exposure time (*h*).

2.4. Electrochemical measurements

The electrochemical experiments were carried out using Potentiostat/Galvanostat having a Gamry framework system based on ESA400. The three-electrode cell consist of mild steel specimens of 1.0 cm^2 area exposed as working electrode, a high purity platinum foil as counter electrode and saturated calomel electrode (*SCE*) as a reference electrode respectively. All potentials were measured versus *SCE* (saturated calomel electrode). Gamry applications include software *EIS300* for electrochemical impedance, *DC105* for corrosion measurements. Echem Analyst version 5.50 software package was used for data fitting. It enables the fitting of the experimental results to a pure electronic model for representing the electrochemical system under investigation. Prior to the electrochemical measurements the working electrode was immersed in 1 M HCl in absence and presence inhibitor for 30 minutes to stabilization of the *OCP w.r.t. SCE*. All the impendence measurements were performed

under a potentiodynamic condition from 100,000 *Hz* to 0.01 *Hz* with amplitude of 10 *mV* peak-to-peak. The polarization measurements were performed by changing the electrode potential automatically from -250 to +250m*V* vs. *OCP* at a scan rate of 1 mV s^{-1}. The linear Tafel segments of anodic and cathodic curves were extrapolated to the corrosion potential to obtain corrosion current densities (I_{corr}). The linear polarization study was carried out from cathodic potential of −20m*V* vs. *OCP* to an anodic potential of +20m*V* vs. *OCP* at a scan rate 0.125m*V* s^{-1} to study the polarization resistance (R_p).

3. RESULTS AND DISCUSSIONS:

3.1 Weight loss studies:

3.1.1 Effect of inhibitor concentration

The corrosion parameters obtained from weight loss measurements are given in table 1 and variation of inhibition efficiency (η%) with inhibitor concentration from 2ppm to 10 ppm is shown in Figure 2 (a). From results it is observed that the maximum inhibition efficiency (97%) was achieved at a concentration of 10 ppm and further increase in concentration did not cause any appreciable change in efficiency of inhibitor. The inhibition efficiency (η%) of investigated inhibitor was determined using following equation:.

$$\eta\% = \frac{w_o - w_i}{w_o} \times 100 \qquad\qquad (4)$$

where w_0 and w_i are the weight loss value in the absence and presence of inhibitor, respectively
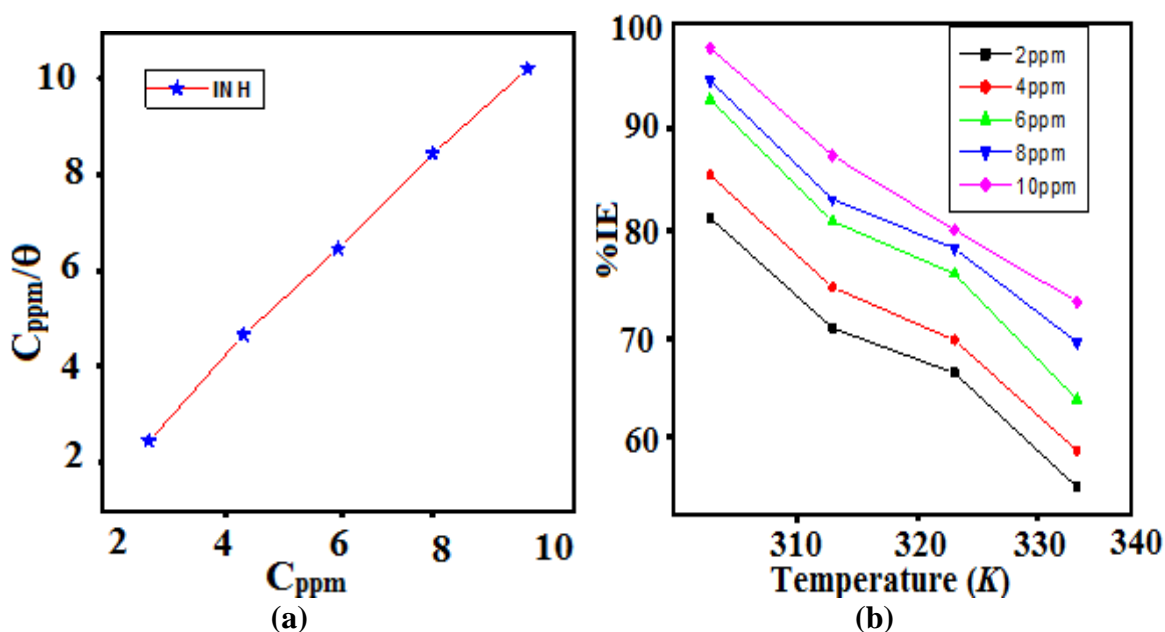
Figure 1. Variation of inhibition efficiency (η%) of heterocyclic inhibitor in 1 M HCl with (a) Inhibitor concentration (b) Temperature of solution

3.1.2 Effect of temperature:

The effect of temperature on inhibition efficiency is shown in Figure. 2 (b). It is clear that inhibition efficiency of investigated inhibitor decreases from 98% to75% with increasing temperature from 308ºK to 338ºK. The decrease in inhibition efficiencies might be due to the desorption inhibitor from mild steel surface [20]. At higher temperature, more desorption of inhibitors takes place and greater surface area of metal comes in contact with acid environment, resulting in an increase in corrosion rate.

Table 1. Corrosion rate (C_R), Surface coverage (θ) and corrosion inhibition ($\eta\%$) for mild steel in 1M HCl in absence and in presence of different concentration of inhibitor from weight loss measurements at 308 K.

Inhibitor	*C_{inh}* $(mg\ L^{-1}/\ Mx10^{-5})$	*C_R* $(mg\ cm^{-2}\ h^{-3})$	*Surface coverage* *(θ)*	*η(%)*
Blank	0.0/0.0	81.25	……	……
	2.00/1.0	15.21	0.812	81.2
	4.00/1.8	11.87	0.853	85.3
INH	6.00/2.7	5.93	0.926	92.6
	8.00/3.7	4.45	0.945	94.5
	10.0/4.6	1.85	0.977	97.7

3.2.3 Thermodynamic parameters and adsorption isotherm

In order to obtain more information about the interaction between the inhibitor molecule and the metal surface, different adsorption isotherms were tested. Langmuir adsorption isotherm was found to be best fit which assumes that the solid surface contains a fixed number of adsorption sites and each site holds one adsorbed species [21]. Langmuir isotherm give a straight line between log *(θ/1-θ)* and log *C (M)* having regression coefficient (R^2) 0.9997 as shown below in Figure 2 (a).

The corrosion rate (C_R) depends upon temperature and this temperature dependence corrosion rate of a chemical reaction can be expressed by following Arrhenius equation [22].

$$\log(C_R) = \frac{-E_a}{2.303RT} + \log \lambda \qquad (5)$$

where *E*a is activation energy for the corrosion of Mild Steel in 1 M HCl, λ pre-exponential factor, *R* is the gas constant, *A* the Arrhenius pre-exponential factor and *T* is the absolute temperature. The Arrhenius plots for mild steel immersed in 1M HCl in inhibitor-free and with inhibitor solution is depicted in Figure 2 (b). The plots obtained were straight lines and apparent activation energies (E_a) at optimum concentration of inhibitors were determined by linear regression between log C_R vs. 1/T and listed in Table 2. All the linear regression coefficients are close to unity. An inspection of Table 2 shows that E_a values (47.73-930.1 kJ mol^{-1}) at different concentration of inhibitor are greater than that of without inhibitor (28.48 kJ mol^{-1}). The increase in E_a resulted either due to physical adsorption in first stage [23-26] or due to decrease in the adsorption of inhibitor molecules on the mild steel surface

with increase in temperature [27]. The higher values of E_a in the presence of inhibitor are due to increase thickness of the double layer which retards the corrosion process [28].
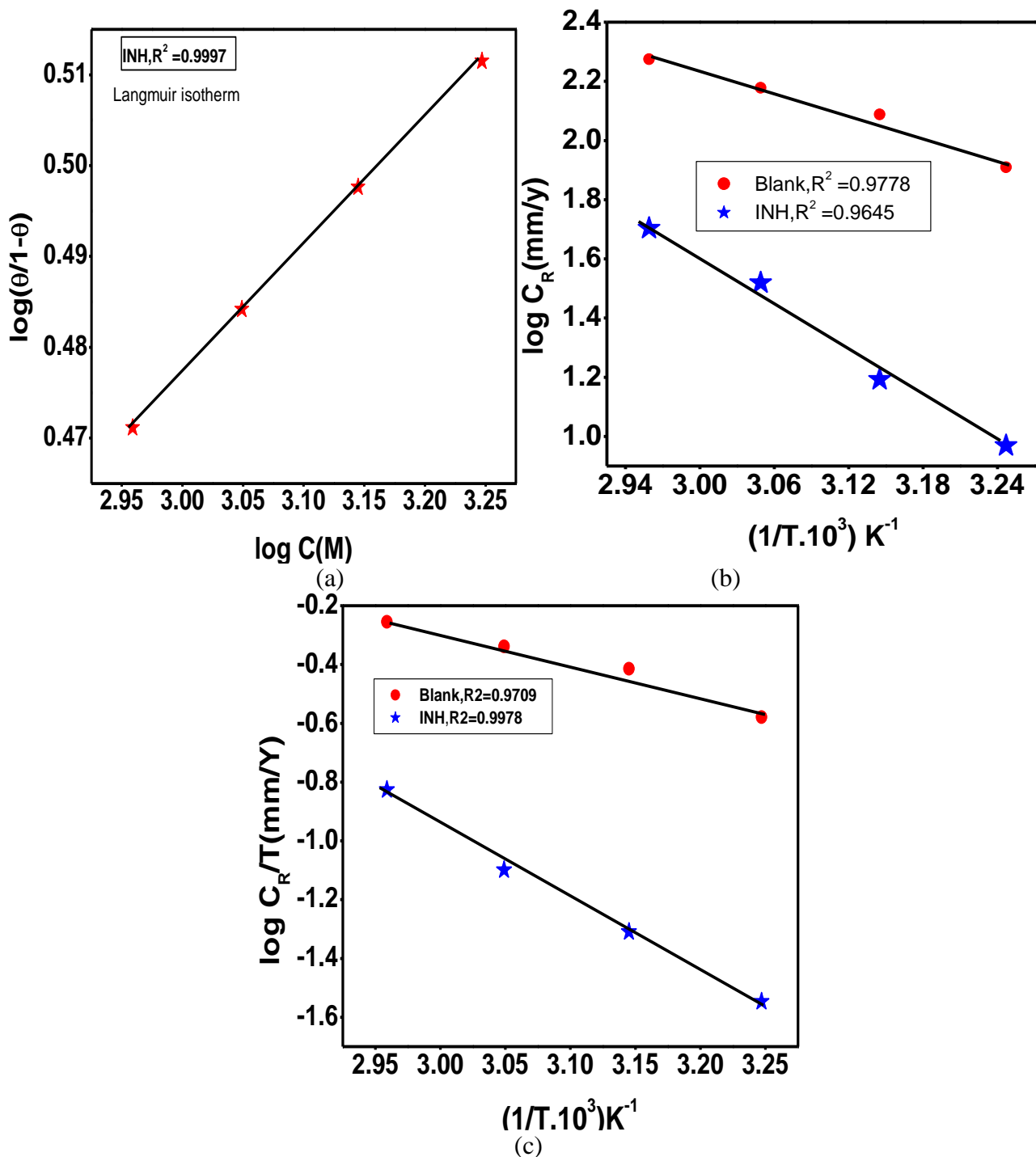
Figure 2.(a-c)(a) Langmuir adsorption isotherm **(b)** Arrhenius plot of log C_R Vs 1/T (c) Arrhenius plot of log C_R/T Vs *1/T*

The ΔH^* (enthalpy of activation) and ΔS^* (entropy of activation) can be calculated by given equation [29].

$$C_R = \frac{RT}{Nh}\exp\left(\frac{\Delta S^*}{R}\right)\exp\left(-\frac{\Delta H^*}{RT}\right) \qquad (6)$$

where h is Plank's constant, N is Avogadro's number, ΔS^* is the entropy of activation and ΔH^* is the enthalpy of activation. Figure 2 (c). Shows the plot between log C_R/T vs. $1/T$. The plots obtained was straight lines and the values of ΔH^* are calculated from their gradient ($\Delta H^* = \_\text{slope}/2.303R$) and ΔS^* from intercept [log(R/Nh) + ($\Delta S^*/2.303R$)]. The calculated data are listed in Table 2. Inspection of the data reveals that the ΔH^* values for dissolution of mild steel in 1M HCl in presence of inhibitor are higher (44.94– 90.51 kJ mol^{-1}) than that in absence of inhibitor (26.04 kJ mol^{-1}).The positive sign and higher value of ΔH^* reflected the endothermic nature of mild steel dissolution process, meaning that dissolution of mild steel is difficult in presence of inhibitor [30]. The shift towards positive value of entropies (ΔS^*) shows that the activated complex in the rate determining step represents dissociation rather than association, meaning that disordering increases on going from reactants to the activated complex[31].

Table 2. Thermodynamic parameters for mild steel in 1M HCl in absence and presence of different concentration of inhibitor.

Thermodynamical parameters					
Inhibitor Conc(mgL^{-1}) /M x10^{-5}	E_a (kJ mol^{-1})	ΔH (kJ mol^{-1})	ΔS (kJ mol^{-1})	K_{ads} (M-1 10^3)	-ΔG (M-1 10^3)
Blank	28.48	26.04	-148.9	…..	…
2.00/1.0	47.73	44.94	-75.83	2.98	31.96
4.00/1.8	51.78	49.60	-62.76	3.74	32.48
6.00/2.7	68.65	64.96	-17.74	6.54	33.59
8.00/3.7	71.03	68.35	4.72	8.40	34.15
10.0/4.6	93.01	90.51	57.38	16.64	35.08

The standard free energy of adsorption, $\Delta G°_{ads}$ and the values of equilibrium constant, K_{ads} at different temperatures can be calculated from the equation.[32]

$$\frac{C_{(inh)}}{\theta} = \frac{1}{K_{(ads)}} + C_{(inh)} \qquad (7)$$

$$\Delta G°_{ads} = -RT\ln(55.5 K_{ads}) \qquad (8)$$

Generally, the values of $\Delta G°_{ads} \leq -20$ kJ mol^{-1} signify physisorption, and values more negative than -40 kJ mol^{-1} support chemisorption [33]. For investigated compound the calculated values of $\Delta G°_{ads}$ are in the range of -31.96 to -35.08 KJ mol^{-1} at different concentration of inhibitor this result indicates that the adsorption of the inhibitor on mild steel surface involves both physical as well as chemical adsorption [34,35].

3.2 Electrochemical measurements

3.2.1. Potentiodynamic polarization measurements

Polarization measurements were carried out in order to gain knowledge concerning the kinetics of the cathodic and anodic reactions Polarization curves of the mild steel electrode in 1.0 M HCl in absence and at different concentrations of inhibitor is shown in Figure 3. The values of corrosion potential (E_{corr}) and corrosion current density (I_{corr}), obtained by extrapolation of the Tafel lines. The cathodic and anodic Tafel slope (β_c and βa respectively), and corresponding inhibition efficiency ($\eta\%$) at different concentrations of inhibitor in 1 M HCl, are given in Table 3.. From table it is clear that inhibition efficiency increases with increasing concentration and maximum efficiency was obtained was 97% at 10 ppm concentration.
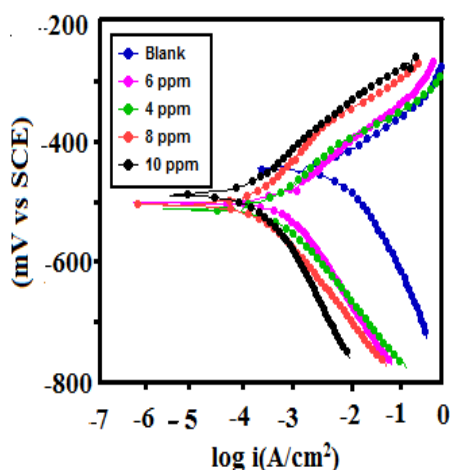
Figure 3. Tafel polarization curves for corrosion of mild steel in 1 M HCl in the absence and presence of different concentrations of inhibitor

Table 3. The Potentiodynamic polarization parameters and corresponding efficiencies in 1 M HCl at different concentration of inhibitor.

Tafel Polarization					
Inhibitor Conc(mgL^{-1}) /M x10^{-5}	*E_{corr}* *(mV vs. SCE)*	*I_{corr}* *(μA cm-2)*	*β_a* *(mV/dec)*	*β_c* *(mV/dec)*	*$\eta\%$*
Blank	-445	1150	70	114	….
4.00/1.8	-501	200	93	150	81.81
6.00/2.7	-512	107	97	103	92.27
8.00/3.7	-505	59	115	112	94.61
10.0/4.6	-488	54	91	119	95.03

The addition of inhibitor did not cause any significant change in E_{corr} suggesting that this is a mixed type inhibitor [36-37]. The adsorbed protective film of inhibitor on the mild steel surface retarded corrosion by blocking the reaction sites of the mild steel. In this way, actual surface area available for H^+ ions is decreased while the actual reaction mechanism remains unaffected [38].

3.2.2 Electrochemical Impedance Spectroscopy

The Impedance method provides information about the electrode kinetics and simultaneously about surface property of investigated system. More ever the shape of impedance gives mechanistic information. The Impedance method is widely used for investigation of corrosion inhibition processes [39]. Nyquist and Bode plots of mild steel in 1M HCl in absence and presence of different concentration of inhibitor are depicted in figure. 4(a) and 4 (b) respectively. From Figure.4 (b) it is clear that a high frequency (*HF*) depressed charge-transfer semicircle was observed followed by well-defined loop in low frequency (*LF*) region.

The Nyquist plots are semicircles and at high frequencies it can be associated to charge transfer resistance for relaxation of electrical double layer. The low frequency loop is attributed to diffusion mass transport from the surface [40–42]. The depressed semi-circle is the characteristic of solid electrodes and often refers to the frequency dispersion which arises due to the roughness and inhomogeneities of the surface [43]. It is worth noting that the change in concentration of inhibitor compound did not alter the shape of the impedance curves, suggesting a similar mechanism of the inhibition. The electrochemical impedance parameters, including R_s, R_{ct}, Y^0 and n, obtained from fitting the recorded EIS using the electrochemical circuit [Figure 4(c)], are listed in Table 4. It can be observed that the charge transfer resistance (R_{ct}) increases with increase in concentrations of inhibitor.

(a)   (b)

(c)
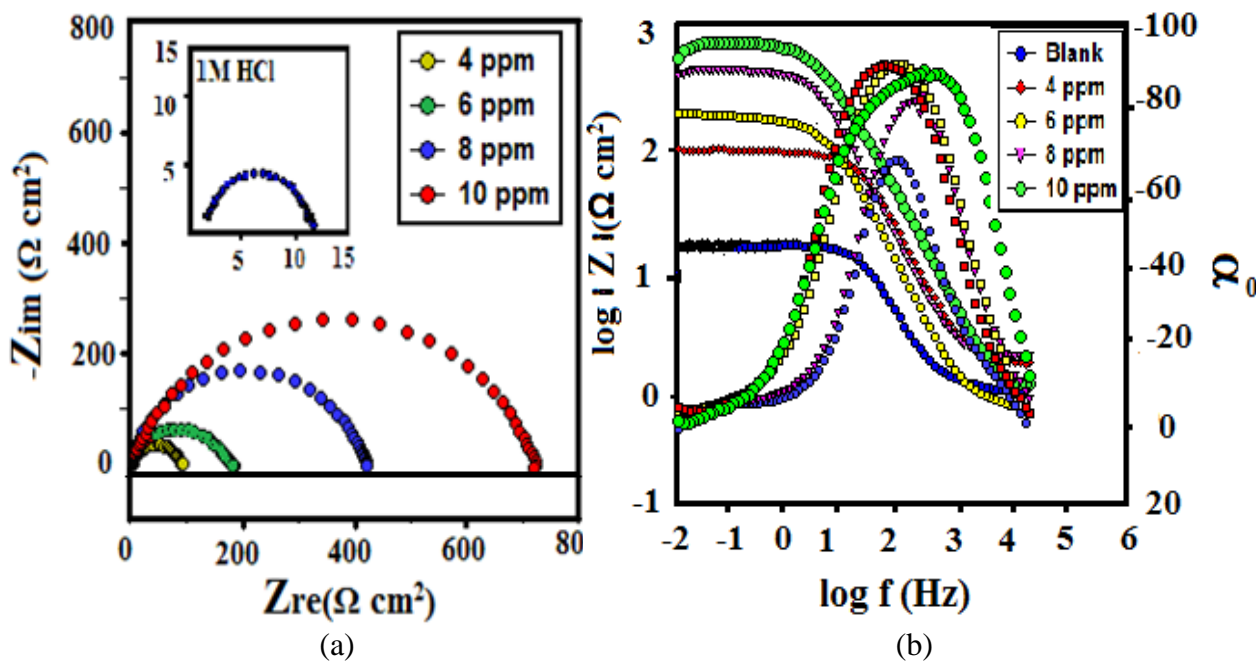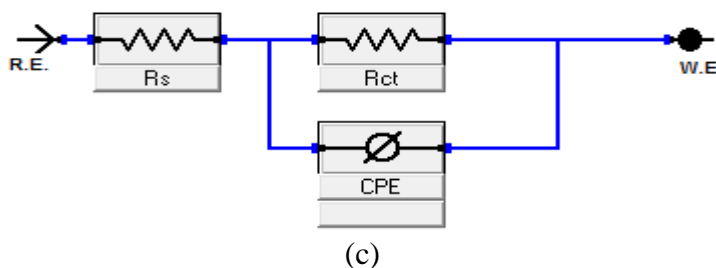
Figure 4(a-c) (a) Nyquist plot in absence and presence of different concentrations of inhibitor (b) Bode plot in absence and presence of different concentrations of inhibitor (c) Equivalent circuit used to fit the impedance data

In the bode plot, phase angle (α^0) at high frequencies provided a general idea of inhibition performance. Examining the phase angle vs. log freq. curves. it is obvious that the most rapid relaxation process occurs at frequencies in the vicinity of 10^4 Hz .The aforementioned relaxation process is associated with the double layer capacitance. At higher frequency greater phase angle suggests the more capacitive electrochemical behavior [44]. The phase angles with smaller values indicate higher surface roughness.

Table 4. The Electrochemical Impedance and Linear polarization parameters and corresponding efficiencies 1 M HCl at different concentration of inhibitor.

Electrochemical Impedance Parameters								*Linear Polarization*	
Inhibitor Conc(mgL^{-1})	R_s (Ω)	R_p (Ω cm^2)	R_{ct} ($\Omega-1$ sn/cm^2)	*n*	Y^0 (μF cm^{-2})	C_{dl}	$\eta\%$	R_p	$\eta\%$
Blank	1.12	12.92	11.8	0.827	249.8	85.08	….	15.09	…….
4	1.476	87.3	85.8	0.858	196.3	104.9	86.24	93.8	85.97
6	0.657	168.5	168.8	0.866	185.7	96.45	93.36	196.9	93.37
8	1.647	414	412.3	0.876	105.0	52.45	97.13	400.3	96.71
10	0.838	711	710.1	0.82	68.24	27.47	98.33	498.6	97.36

The continuous increase in the phase angle shift Figure 4(b) correlating with the increase of inhibitor adsorbed on mild steel surface. The equivalent circuit proposed to represent the corrosion of mild steel electrode in 1.0 M HCl solution, is shown in the Figure. 4(c). Where Rs is the solution resistance, Rct is the charge transfer resistance and C_{dl} is the double-layer capacitance. A constant phase element (*CPE*) is substituted for the capacitive element to give a more accurate fit [45]. The introduction of such a *CPE* is often used to interpret data for rough solid electrodes. The Constant phase element is a special element which exhibits more complicated frequency response than a simple undistributed *RC* time constant process [46]. Its impedance is expressed by the equation as,

$$Z_{CPE} = Q^{-1}(j\omega)^{-n}$$ (9)

where Q^{-1} is the *CPE* coefficient, ω is the angular frequency and *j* is imaginary unit and *n* is a *CPE* exponent (phase shift) which can be used as a gauge of the heterogeneity or roughness of the

surface. It can seen from Table 4, the R_{ct} values increased with increasing the concentration of the inhibitor, indicated that corrosion process mainly controlled by a charge transfer mechanism. The change of C_{dl} values can be related to the gradual replacement of water molecules by inhibitor molecules on the surface which decreases the number of actives sites necessary for corrosion reaction [47] On the other hand the values of C_{dl} decrease with an increase in the inhibitor concentration. The double layer between the charged metal surface and the solution is considered as an electrical capacitor i.e. the adsorption of inhibitors on the electrode surface mild steel may be attributed to the formation of a protective layer on the surface [48, 49].

3.2.3 Linear polarization method.

The inhibition efficiencies and polarization resistance (Rct) parameters are presented in Table 4.The values calculated by Tafel polarization and EIS data shows good agreement with the results obtained from linear polarization resistance. The Linear polarization parameter also shows that on increasing concentration the inhibition efficiency also increases.

4. MECHANISM OF INHIBITION

The results obtained from different electrochemical and weight loss methods shows that investigated inhibitor, inhibits corrosion of mil steel in 1M HCl by getting adsorbed on its surface. However adsorption of organic inhibitor cannot be considers as purely physical or purely chemical phenomenon. The adsorption mechanism is influenced by nature and charge on metal surface and chemical structure of inhibitors. The charge on metal surface is due to electric field which emerges at the metal/electrolyte interface. It is well-known that mild steel specimens are positively charged with respect to the potential of zero charge (*PZC*) in acid solutions [50]. The inhibitor may adsorb on the metal/acid solution interface by:

(I) electrostatic interaction of protonated inhibitor molecules with already adsorbed chloride ions (physisorption),

(II) unshared electron pairs of heteroatoms and vacant d-orbital of Fe surface atoms (chemisorptions), or

(III) interaction of d-electron of iron surface atom to the vacant orbital of inhibitor molecule (retro-donation)

(IV) A combination of (I-IV) [51-53]

The schematic illustration of different modes of adsorption on metal/acid interface is shown in Figure 5. It should be noted that the molecular structure of protonated inhibitor remains unchanged with respect to their neutral form, the N-atoms on the ring remaining strongly blocked, so when protonated inhibitor adsorbed on metal surface, coordinate bond may be formed by partial transference of electrons from the hetero-atoms to the metal surface.
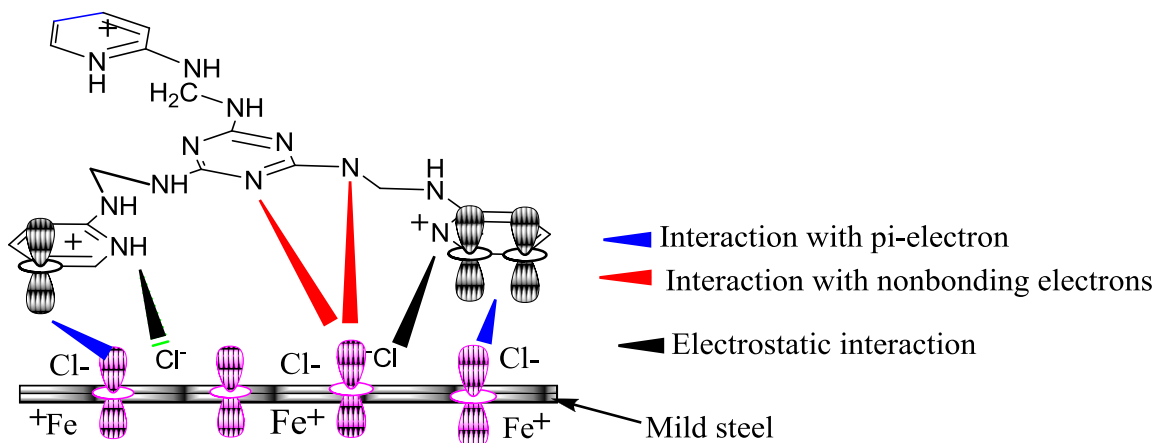
Figure 5. The schematic illustration of different modes of adsorption by inhibitor on mild steel 1 M HCl interface

In aqueous solution of 1M HCl inhibitor molecule may adsorb through protonated heteroatoms and already adsorbed Cl^- on mild steel surface. Initially, the protonated form of inhibitor molecules in acid medium start competing with H^+ ions for electrons on mild steel surface. After release of H_2 gas, the cationic form of inhibitors returns to its neutral form and heteroatoms with free lone pair electrons promote chemical adsorption. The accumulation of electrons on mild steel surface render it more negative and to relieve the metal from extra negative charge the electron from the d-orbital of Fe might be transferred to the vacant π^* (antibonding) orbital of inhibitor molecules (retrodonation) and hence strengthen adsorption on metal surface.

5. CONCLUSIONS

From above study it is concluded that:

1. The N^2,N^4,N^6-tris((Pyridin-2-ylamino)methyl)-1,3,5-triazine-2,4,6-triamine is a good inhibitor for corrosion of mild steel in 1M HCl solution. The maximum efficiency was found be 97% at 10 ppm concentration.

2. The adsorption of inhibitor molecule on mild steel surface obeyed the Langmuir isotherm.

3. The Potentiodynamic studies reveal that inhibitor is a mixed type inhibitor i.e. it affected both cathodic and anodic reactions.

4. The negative values of ΔG shows that adsorption of inhibitor on mild steel is a spontaneous

5. The results obtained from weight loss and electrochemical methods are in good agreement

References

1. N. A Negm, N. G. Kandile, I. A. Aiad, M. **A.** Mohammad *Colloids Surf.*, 391(2011) 224-233
2. H. Ashassi-Sorkhabi, D. Seifzadeh, M. G. EN. Hosseini *Corros. Sci.* 50 (2008) 3363-3370
3. F Bentiss, C. Jama, B. Mernari, H. E. Attari, L. E. Kadi, M .Lebrini, M. Traisnel, M. Lagrenee *Corros. Sci.* 51 (2009) 1628-1635

4.   D. K. Yadav, B. Maiti, M.A. Quraishi. *Corros. Sci.* 52 (2010) 3586-3598
5.   A. M. Fekry, M. A. Ameer *Int. J. Hydrogen Energy* 35(2010) 7641-7651.
6.   P. Lowmunkhong, D. Ungthararak, P. Sutthivaiyakit . *Corros. Sci.* 52(2010) 30-36
7.   B. D. M. Mert E. Mert ru, G. Kardas, B.Yazıcı *Corros. Sci.* 53(2011) 4265-4272
8.   M. Mahdavian, S. Ashhari *Electrochimica Acta*, 55 (2010) 1720-1724.
9.   A. Doner, R. Solmaz, M. Ozcan, G. Kardas *Corros. Sci.,* 53(2011) 2902-2913
10. M. A. Ameer, A. M. Fekry *Int. J. Hydrogen Energy* 35(2010) 11387-11396.
11. A. M. Fekry, M. A. Ameer *Int. J. Hydrogen Energy*, 36(2011), 11207-11215
12. G.J. Village, F. Li, L. Yongji W. Li, . (2007).*Xinjiang Oil and Gas,* 3
13. W. Ziang and Y. Jing. (1999). *Oilfield Chemistry*, 2
14. M.A. Quraishi, I. Ahmad, A.K. Singh, S.K. Shukla, B. Lal, V. Singh. *Mater. Chem. Phy.*, 112 (2008) 1035-1039.
15. F. Bentiss, M. Lagrenee, M. Traisnel, J. C. Hornez *Corrosion*, *41*(4) (1999) 789-803.
16. F.B. Growcock, W.W. Frenier, P.A. Andreozzi *Corrosion. 45*(12) (1989) 1007-1012
17. I. Lukovits, E. Kalman, G. Palinkas, *Corrosion*, *51*(3) (1995) 201-205.
18. R.C. Ayers, N. Jr. Hackerman *J. Electrochem. Soc.*, *110*(6) (1963) 507-513.
19. C. Verma M.A.,Quraishi,E.E. Ebenso, *Int. J. Electrochem. Sci.*,8 (2013)7401 - 7413
20. I. Ahamad. R. Prasad and M.A. Quraishi *Corros. Sci.* 52, (2010) 3033-3041.
21. A.O. Yuce, R. Solmazb, G. Kardas *Mater. Chem. Phys.* 131 (2012) 615 -620
22. I. Ahamad. R. Prasad and M.A. Quraishi *Corros. Sci.* 52 (2010)   1472– 1481.
23. C.S. Venkatachalam, S.R, Rajagopalan, M.V.C. Sastry *Electrochim. Acta* 26(1981)   1219–1224
24. E.A. Noor, A.H. Al-Moubaraki, Mater. Chem. Phys. 110 (2008) 145–154.
25. L. Larabi, Y. Harek, O. Benali, S. Ghalem, Prog. Org. Coat. 54 (2005) 256–262.
26. L. Larabi, O. Benali, Y. Harek, Mater. Lett. 61 (2007) 3287–3291.
27. T. Szauer, A. Brandt, Electrochim. Acta 26 (1981) 1209–1217.
28. A.O. Yuce, G. Kardas *Corros. Sci.* 58(2012) 86 -94
29. Deng X. Li, S., Fu H., Mu G*, Corros.   Sci*. 50 (2008)2635– 2645
30. N.M. Guan, L. Xueming, L. Fei, Mater. Chem. Phys. 86 (2004) 59–68.
31. M.A. Quraishi, A. Singh, V.K. Singh, D.K. Yadav, A.K. Singh, *Mater. Chem. Phys.,* 122   (2010) 114
32. I. Ahamad. R. Prasad and M.A. Quraishi. *Corros. Sci.* 52 (2010) 1472-1481
33. A. M. Fekry, R. R. Mohamed *Electrochim. Acta*, 55(2010) 1933-1939
34. A. Doner, R. Solmaz, M. Ozcan, G. Kardas *Corros. Sci.* 53 (2011)   2902 -2913
35. P.R. Roberge (2000) Handbook of Corrosion Engineering*, McGraw-Hill, New York,*
36. E. S. Ferreira, C. Giacomelli, F. C., Giacomelli, A. Spinelli *Mater. Chem. Phys.*, 83(2004) 129-134
37. O. Riggs, L.Jr. Corrosion Inhibitors, 2nd ed.; C. C. Nathan (1973) Houston, *TX, USA*,; p 109.
38. R. Solmaz, G. Kardas, M. Culha, B. Yazici, M. Erbil *Electrochim. Acta*, 53(2008) 5941.
39. A. Y. Musa, A. A. H. Kadhum, A. B. Mohamad, M. S Takriff, A. R. Daud, S. K. A. Kamarudin *Corros. Sci.*, 51 (2009)   2393−2399
40. K.Juttner *Electrochim. Acta* 35 (1990) 1501−1508.
41. C.T. Wang, S.H. Chen, H.Y. Ma, C.S. Qi *J. Appl. Electrochem.* 33(2003)   179–186
42. K.F. Khaled *Corros. Sci.* 52 (2010) 3225–3234.
43. M. Bouklah, A. Ouassini, B. Hammouti, A. El Idrissi *Appl. Surf. Sci.* 252(2006) 2178
44. A. Popova, M. Christov *Corros. Sci.* 48 (2005) 3208-3221
45. M. W. Kendig, E. T. Allen, F. Mansfeld *J. Electrothem. Soc.* 131(1984)   935
46. F. Mansfeld, S. L. Jeanjaquet, M. W. Kendig *Corros. Sci.* 26(1986) 735-742
47. T. Zhao and G. Mu *Corros. Sci.* 41(1999) 1937-1944
48. F. Bentiss, M. Traisnel, M. Lagrenée *Corros. Sci.* 42(2000) 127-146
49. H.J. Flitt, and D. P. Schweinsberg, *Corros. Sci.*   47(2005) 2125-2156
50. S. Deng, X. Li, H. Fu *Corros. Sci*, 53(2011)760-768

51. D.P. Schweinsberg, G.A George, A.K. Nanayakkara, D.A. Steiner *Corros. Sci.* 28(1988) 33-42
52. H. Shorky, M. Yuasa, R.M. Sekine Issa, H.Y. El-Baradie, G.K. Gomma *Corros. Sci.*40(1998) 2173-2186
53. A.K. Singh, M.A. Quraishi *Corros. Sci.* 52(2010) 152-160